

# Magnetic properties and $^{151}\text{Eu}$ Mössbauer effects of mixed valence europium copper sulfide, $\text{Eu}_2\text{CuS}_3$

Fumito Furuuchi, Makoto Wakeshima, and Yukio Hinatsu\*

*Division of Chemistry, Graduate School of Science, Hokkaido University, Sapporo 060-0810, Japan*

Received 10 November 2003; accepted 22 April 2004

Available online 21 September 2004

## Abstract

Ternary europium copper sulfide  $\text{Eu}_2\text{CuS}_3$  have been investigated by X-ray diffraction,  $^{151}\text{Eu}$  Mössbauer spectroscopy, magnetic susceptibility, magnetization, and specific heat measurements. In this compound,  $\text{Eu}^{2+}$  and  $\text{Eu}^{3+}$  ions occupy two crystallographically independent sites. The  $^{151}\text{Eu}$  Mössbauer spectra indicate that the  $\text{Eu}^{2+}$  and  $\text{Eu}^{3+}$  ions exist in the molar ratio of 1:1, and the Debye temperatures of  $\text{Eu}^{2+}$  and  $\text{Eu}^{3+}$  are 180 and 220 K, respectively. In its magnetic susceptibility, the divergence between the zero-field cooled and field cooled susceptibilities appears below 3.4 K. The specific heat has a  $\lambda$ -type anomaly at the same temperature. From the field dependence of magnetization at 1.8 K, the  $\text{Eu}^{2+}$  ion was found to be in the ferromagnetic state with the saturation magnetization  $M_S = 6.7 \mu_B$ .

© 2004 Elsevier Inc. All rights reserved.

**Keywords:** Magnetic properties; Mössbauer spectroscopy; Magnetic susceptibility; Specific heat; Europium; Copper; Sulfide

## 1. Introduction

Ternary europium copper sulfide  $\text{Eu}_2\text{CuS}_3$  has been reported to crystallize in the orthorhombic structure with space group *Pnma* [1]. The schematic structure of  $\text{Eu}_2\text{CuS}_3$  is illustrated in Fig. 1. This compound has the formal oxidation state of  $\text{Eu}^{2+}\text{Eu}^{3+}\text{Cu}^+\text{S}_3^{2-}$  and the  $\text{Eu}^{2+}$  and  $\text{Eu}^{3+}$  ions occupy crystallographically different sites. In the case of sulfides, the mixed-valence compounds show an interesting electronic behavior as the valence state and the magnetic interaction. For example,  $\text{Eu}_3\text{S}_4$  has the Verwey transition at 186 K [2] and the ferromagnetic transition at 3.1 K [3].  $\text{EuPd}_3\text{S}_4$  shows an electron hopping between  $\text{Eu}^{2+}$  and  $\text{Eu}^{3+}$  and has the antiferromagnetic transition at 3 K [4].  $\text{Eu}_5\text{Sn}_3\text{S}_{12}$  is metamagnetic and has two field-dependent antiferromagnetic phases at low temperatures [5].

Generally, the divalent state of Eu is stable in sulfides, but some compounds contain trivalent europium. Flahaut noted that these were classified into two types [6]. In the case that compounds containing only  $\text{Eu}^{3+}$  ions, there is necessarily a strongly electronegative

anion, or a second weakly electronegative cation. For compounds containing mixtures of  $\text{Eu}^{2+}$  and  $\text{Eu}^{3+}$ ,  $\text{Eu}_3\text{S}_4$  [7] and  $\text{EuPd}_3\text{S}_4$  [4],  $^{151}\text{Eu}$  Mössbauer spectroscopic measurements were performed to investigate the mixed-valence state of Eu. These compounds show the occurrence of the electron transfer and/or the electron hopping between  $\text{Eu}^{2+}$  and  $\text{Eu}^{3+}$ , which may stabilize the  $\text{Eu}^{3+}$  ions. The situation for  $\text{Eu}_2\text{CuS}_3$  is different from the case for the above-mentioned sulfides, i.e.,  $\text{Eu}_2\text{CuS}_3$  has two crystallographically distinguishable sites for  $\text{Eu}^{2+}$  and  $\text{Eu}^{3+}$  ions. However, none of the studies on the electronic and magnetic properties of this mixed valence compound have been carried out.

In this study, we synthesized the polycrystalline samples of  $\text{Eu}_2\text{CuS}_3$  and have measured the magnetic susceptibility, magnetization, specific heat measurements and  $^{151}\text{Eu}$  Mössbauer spectroscopy. The results will be discussed in detail.

## 2. Experimental

A ternary europium copper sulfide,  $\text{Eu}_2\text{CuS}_3$ , was synthesized by a solid-state reaction. Europium monosulfide (EuS), copper powders, and sulfur were used as

\*Corresponding author. Fax: +81-11-706-2702.

E-mail address: [hinatsu@sci.hokudai.ac.jp](mailto:hinatsu@sci.hokudai.ac.jp) (Y. Hinatsu).

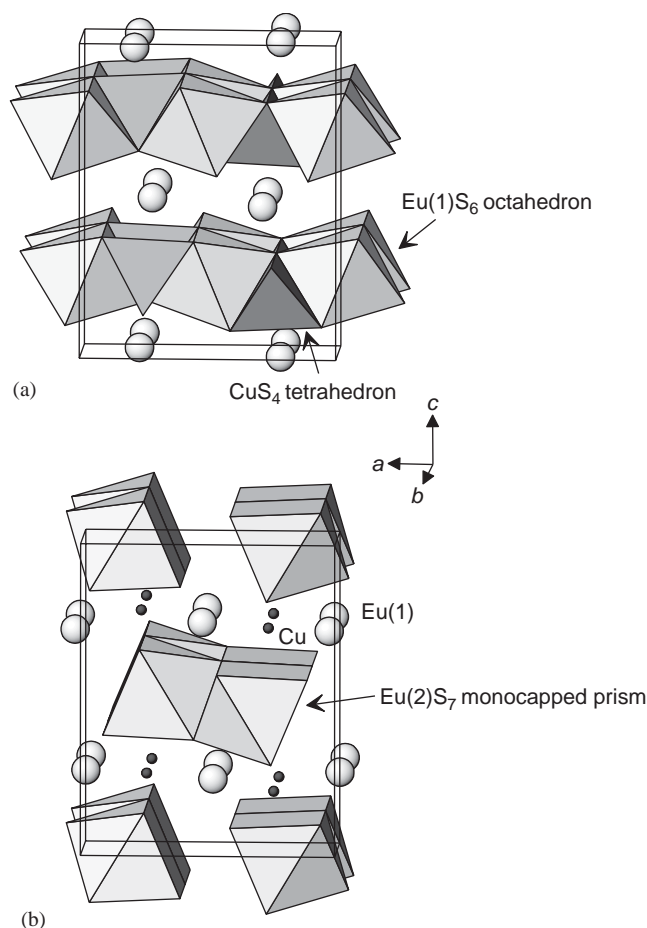


Fig. 1. Polyhedral representation of the  $\text{Eu}_2\text{CuS}_3$  structure. (a)  $\text{CuEu(1)S}_3$  layers composed of  $\text{Eu(1)S}_6$  octahedra and  $\text{CuS}_4$  tetrahedra. (b) The double chains of the  $\text{Eu(2)S}_7$  monocapped trigonal prisms with  $\text{Eu(1)}$  and  $\text{Cu}$  represented by the larger and the smaller spheres.

starting materials. To obtain the europium monosulfide, europium sesquioxide ( $\text{Eu}_2\text{O}_3$ ) was heated on a graphite boat at 1273 K in a flow of the mixed gas of  $\text{CS}_2$  and  $\text{N}_2$ , which was obtained by bubbling the  $\text{N}_2$  gas through liquid  $\text{CS}_2$  at room temperature. Stoichiometric mixtures of the starting materials were ground and pressed into a pellet, and then heated in a quartz ampoule. The inner wall of the ampoule was, in advance, coated with a carbon film by decomposing benzene. The reaction was carried out at 1173 K for 12 h, with one interval regrinding.

Powder X-ray diffraction measurements were performed with  $\text{CuK}\alpha$  radiation on a Rigaku MultiFlex diffractometer equipped with a curved graphite monochromator. Intensity data were collected by step scanning in the range  $2\theta = 10^\circ - 120^\circ$  at intervals of  $0.02^\circ$ . The structure and lattice parameters were refined with a Rietveld program RIETAN 2000 [8].

The  $^{151}\text{Eu}$  Mössbauer spectra were measured between 15 and 300 K with a Mössbauer spectrometer VT-6000

(Laboratory Equipment Co.) using a radiation source  $^{151}\text{SmF}_3$  (1.85 GBq). The sample lapped in an aluminum foil was cooled down to each temperature and the isomer shift was determined relative to the shift of europium fluoride ( $\text{EuF}_3$ ).

Magnetic susceptibility measurements of the powder sample weighing  $\sim 20$  mg were performed with a SQUID magnetometer (Quantum Design MPMS model) from 1.8 to 300 K. The applied field was 0.1 T. In the neighborhood of the magnetic transition, the magnetic susceptibility was measured under zero-field cooled (ZFC) and field cooled (FC) conditions with 5 mT. The field dependence of magnetization was measured at 1.8 K by changing the applied magnetic field between  $-5$  and 5 T.

The specific heat measurement was carried out using a relaxation technique supplied by commercial specific heat measurement system (Quantum Design, PPMS) in the temperature range from 1.8 to 300 K. The sample in the form of pellet ( $\sim 7$  mg) was mounted on an aluminum plate with apiezon for better thermal contact.

### 3. Results and discussion

The  $\text{Eu}_2\text{CuS}_3$  compound was obtained as a single phase. The X-ray diffraction profile was indexed on an orthorhombic cell with the space group  $Pnma$ , and its crystallographic parameters were refined by the Rietveld method. Fig. 2 shows the X-ray diffraction profile of  $\text{Eu}_2\text{CuS}_3$ . The calculated profile was in good agreement with the observed one ( $R_{\text{wp}} = 8.10\%$ ,  $R_I = 2.95\%$ ). The refined lattice and positional parameters are listed in Table 1, and the selected interatomic distances are listed in Table 2. These values for the lattice parameters and the interatomic distances agree with those reported by Lemoine et al. [1].

The crystal structure of  $\text{Eu}_2\text{CuS}_3$  is shown in Fig. 1. In this structure, the Eu ions occupy two crystallographically independent sites. The  $\text{Eu(1)}$  ions are coordinated

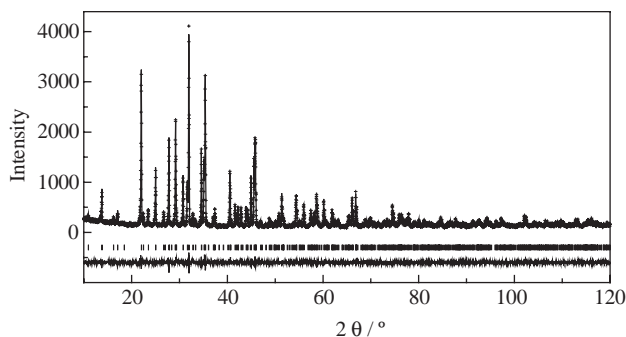


Fig. 2. Powder X-ray diffraction patterns and Rietveld refinements for  $\text{Eu}_2\text{CuS}_3$ . The bottom trace is a plot of the difference between observed + (cross markers) and calculated (solid line) intensities. All allowed Bragg reflections are shown by vertical lines.

Table 1  
Lattice parameters and atomic positions of  $\text{Eu}_2\text{CuS}_3$

Space group: $Pnma$					
$Z = 4$					
$a = 10.3596(2) \text{ \AA}, b = 3.9586(1) \text{ \AA}, c = 12.8194(3) \text{ \AA}$					
Atom	Site	$x$	$y$	$z$	$B (\text{\AA}^2)$
Eu(1)	4c	0.0164(2)	1/4	0.7374(1)	0.46(5)
Eu(2)	4c	0.7801(2)	1/4	0.0014(2)	0.55(5)
Cu	4c	0.2321(4)	1/4	0.2225(3)	0.80(9)
S(1)	4c	0.0505(6)	1/4	0.1157(5)	0.55(17)
S(2)	4c	0.4068(7)	1/4	0.1021(5)	0.30(16)
S(3)	4c	0.2635(7)	1/4	0.8280(5)	0.57(16)

$$R_{\text{wp}} = \left[ \frac{\sum w(|F_o| - |F_c|)^2}{\sum w|F_o|^2} \right]^{1/2} = 8.10\%$$

$$R_I = \frac{\sum |I_o - I_c|}{\sum I_o} = 2.95\%$$

$$R_F = \frac{\sum |F_o - F_c|}{\sum F_o} = 2.13\%$$

Table 2  
Selected interatomic distances ( $\text{\AA}$ ) of  $\text{Eu}_2\text{CuS}_3$

Eu(1)–S(2)	2.795(5) × 2
Eu(1)–S(3)	2.795(8)
Eu(1)–S(3)	2.812(7)
Eu(1)–S(1)	2.818(5) × 2
Eu(2)–S(3)	2.985(5) × 2
Eu(2)–S(1)	3.041(5) × 2
Eu(2)–S(2)	3.070(5) × 2
Eu(2)–S(1)	3.121(6)
Cu–S(1)	2.344(7)
Cu–S(2)	2.363(7)
Cu–S(3)	2.397(4) × 2

by six sulfur ions and the  $\text{Eu}(1)\text{S}_6$  octahedra share corners along the  $a$ -axis and edges along the  $b$ -axis. The  $\text{Eu}(1)\text{S}_6$  octahedra and  $\text{CuS}_4$  tetrahedra form a  $\text{CuEu}(1)\text{S}_3$  layer perpendicular to the  $c$ -axis. The  $\text{Eu}(2)$  ions are coordinated by seven sulfur ions between the  $\text{CuEu}(1)\text{S}_3$  layers and make the  $\text{Eu}(2)\text{S}_7$  monocapped trigonal prisms. The bases of the  $\text{Eu}(2)\text{S}_7$  monocapped trigonal prisms, S(1), S(2), and S(3), are shared by each other to make a chain along the  $b$ -axis and one corner of this base, S(1), is also coordinated by the  $\text{Eu}(2)$  belonging to the neighboring chain.

The valences of the cations are calculated by the bond valence sum ( $V_i$ ) [9]:

$$v_{ij} = \exp\left(\frac{R_0 - d_{ij}}{b}\right), \quad (1)$$

$$V_i = \sum_j v_{ij}, \quad (2)$$

where  $R_0$  and  $b$  are known as the bond valence parameters of various cations and a constant value

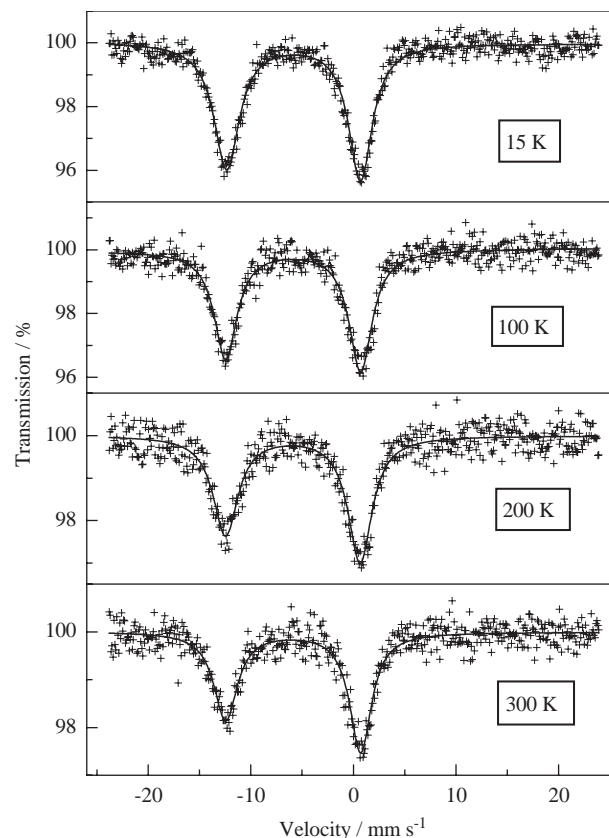


Fig. 3.  $^{151}\text{Eu}$  Mössbauer spectra of  $\text{Eu}_2\text{CuS}_3$  at 15, 100, 200, and 300 K.

(0.37  $\text{\AA}$ ), respectively, and  $d_{ij}$  means the interatomic distance between cation  $i$  and anion  $j$ . The valences of the  $\text{Eu}(1)$ ,  $\text{Eu}(2)$ , and  $\text{Cu}$  ions were determined to be +3.04, +1.73, and +0.971, respectively. This result indicates that the trivalent and divalent europium ions occupy the  $\text{Eu}(1)$  and  $\text{Eu}(2)$  sites, respectively.

Fig. 3 shows the  $^{151}\text{Eu}$  Mössbauer spectra of  $\text{Eu}_2\text{CuS}_3$  between 15 and 300 K. Two absorption peaks appear at ca.  $-12$  and  $0 \text{ mm s}^{-1}$  in these spectra, indicating the presence of the divalent and trivalent  $\text{Eu}$  ions. To simplify this analysis, each peak was fitted with a single Lorentzian. The isomer shifts of  $\text{Eu}^{2+}$  ( $\delta \sim -12.4 \text{ mm s}^{-1}$ ) and  $\text{Eu}^{3+}$  ( $\delta \sim 0.68 \text{ mm s}^{-1}$ ) are nearly constant between 15 and 300 K. It is known that the difference in the isomer shifts between  $\text{Eu}^{2+}$  and  $\text{Eu}^{3+}$  decreases with increasing temperature in mixed valence europium sulfides,  $\text{Eu}_3\text{S}_4$  [7],  $\text{EuPd}_3\text{S}_4$  [4], and  $(\text{EuS})_{1.173}\text{NbS}_2$  [10] because of the electron hopping between  $\text{Eu}^{2+}$  and  $\text{Eu}^{3+}$ . The temperature dependence of the isomer shifts for  $\text{Eu}_2\text{CuS}_3$  means that the electron hopping does not occur in this compound.

Fig. 4 shows the temperature dependence of the absorption area of the intensity curves of the  $\text{Eu}^{2+}$  and  $\text{Eu}^{3+}$  ions. Both intensities decrease monotonously with increasing temperature. The intensities for  $\text{Eu}^{2+}$  and

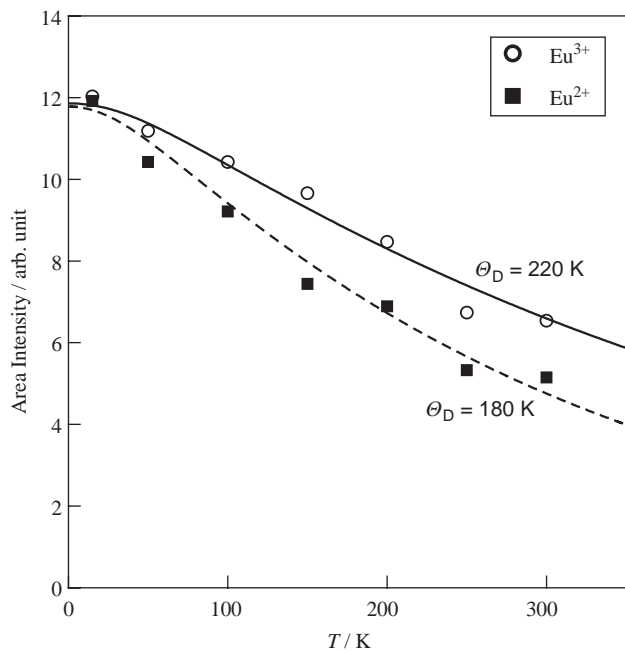


Fig. 4. Temperature dependence of the absorption area of intensities of  $\text{Eu}_2\text{CuS}_3$ . The solid line is the theoretical curve ( $\Theta_D = 180$  K) normalized to  $A(\text{Eu}^{2+})$  at 15 K and the broken line is the theoretical curve ( $\Theta_D = 220$  K) normalized to  $A(\text{Eu}^{3+})$  at 15 K.

$\text{Eu}^{3+}$  are equal at 15 K but the ratio of the intensities for  $\text{Eu}^{2+}$  and  $\text{Eu}^{3+}$  is found to be 2:3 at 300 K. This difference may be due to a difference in the Debye–Waller factors between  $\text{Eu}^{2+}$  and  $\text{Eu}^{3+}$ . The area of the intensity curve is proportional to the recoil-free fraction. The Debye temperatures for  $\text{Eu}^{2+}$  and  $\text{Eu}^{3+}$  are estimated from the recoil-free fraction. The recoil-free fraction is represented by [11]

$$f = \exp \left[ \frac{-6E_R}{k_B\Theta_D} \left\{ \frac{1}{4} + \left( \frac{T}{\Theta_D} \right)^2 \int_0^{\Theta_D/T} \frac{x dx}{(e^x - 1)} \right\} \right], \quad (3)$$

where  $k_B$  is the Boltzmann's constant,  $\Theta_D$  is the Debye temperature, and  $E_R$  is the free-atom recoil energy. The theoretical curves with  $\Theta_D = 180$  K and  $\Theta_D = 220$  K using this equation are in good agreement with the experimental data for  $\text{Eu}^{2+}$  and  $\text{Eu}^{3+}$ . The higher Debye temperature for the  $\text{Eu}(1)$  ion indicates that the  $\text{Eu}^{3+}-\text{S}^{2-}$  bonds in the  $\text{Eu}(1)\text{S}_6$  octahedron are

$$\chi_M(\text{Eu}^{3+}) = \frac{N_A \mu_B^2}{3k_B \gamma T} \frac{24 + (13.5\gamma - 1.5)e^{-\gamma} + (67.5\gamma - 2.5)e^{-3\gamma} + (189\gamma - 3.5)e^{-6\gamma} + \dots}{1 + 3e^{-\gamma} + 5e^{-3\gamma} + 7e^{-6\gamma} + \dots}, \quad (5)$$

stronger than the  $\text{Eu}^{2+}-\text{S}^{2-}$  bonds in the  $\text{Eu}(2)\text{S}_7$  monocapped trigonal prism, which is attributable to the small coordination-number and the short interatomic

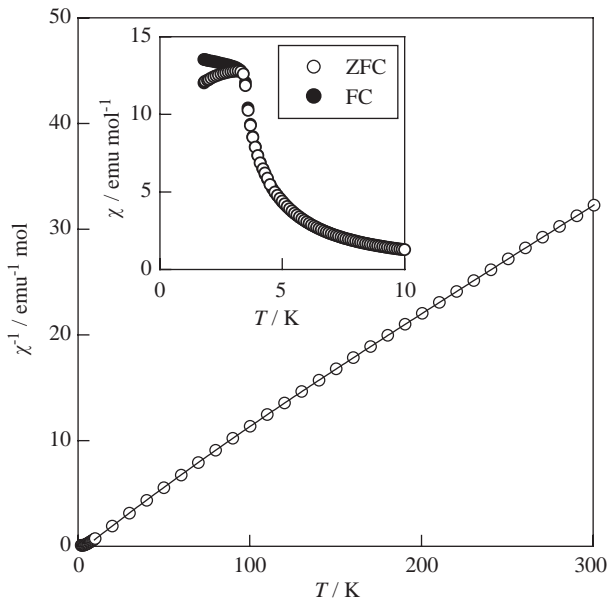


Fig. 5. Temperature dependence of the reciprocal magnetic susceptibility  $\chi^{-1}$  of  $\text{Eu}_2\text{CuS}_3$ . A solid line is the fitting result by using Eq. (4) (see text). The inset shows  $\chi$  of  $\text{Eu}_2\text{CuS}_3$  below 10 K measured in the magnetic field of 5 mT.

distances for  $\text{Eu}(1)\text{S}_6$  as compared with those for the  $\text{Eu}^{2+}-\text{S}^{2-}$  bonds of  $\text{Eu}(2)\text{S}_7$ .

Fig. 5 shows the reciprocal magnetic susceptibilities ( $\chi^{-1}$ ) of  $\text{Eu}_2\text{CuS}_3$  as a function of temperature in the magnetic field of 0.1 T. The molar susceptibilities of  $\text{Eu}_2\text{CuS}_3$  is given by

$$\chi_M = \chi_M(\text{Eu}^{2+}) + \chi_M(\text{Eu}^{3+}) + \chi_0, \quad (4)$$

where  $\chi_0$  is the temperature-independent term containing the diamagnetic term. The ground state of the  $\text{Eu}^{2+}$  ion is  $^8\text{S}_{7/2}$ . Therefore the orbital angular momentum vanishes, and the crystal field does not affect the magnetic properties of  $\text{Eu}^{2+}$  compounds. The magnetic susceptibility ( $\chi_M(\text{Eu}^{2+})$ ) of  $\text{Eu}^{2+}$  is represented by  $N_A \mu_{\text{eff}}^2 / 3k_B(T - \Theta_W)$ , where  $\mu_{\text{eff}}$  is the effective magnetic moment and  $\Theta_W$  is the Weiss constant. The ground state ( $^7F_0$ ) of  $\text{Eu}^{3+}$  is nonmagnetic, and the excited states  $^7F_J$  ( $J = 1, 2, \dots, 6$ ) are close enough to give energy differences comparable to  $k_B T$  at room temperature. Thus, in consideration of the excited states, the magnetic susceptibility of  $\text{Eu}^{3+}$  can be written as

where  $\gamma = \lambda/k_B T$  is 1/21 of the ratio of the over all multiplet width to  $k_B T$  [12]. On the assumption that the screening number is 34, the theoretical value of  $\lambda/k_B$  is

$363 \text{ cm}^{-1}$ . If  $\lambda/k_B$  was fixed to be  $363 \text{ cm}^{-1}$  [12], the values of  $\mu_{\text{eff}}$  and  $\Theta_W$  of  $\text{Eu}^{2+}$  were determined to be  $7.96(1)\mu_B$  and  $+4.74(2)\text{K}$ , respectively. The effective magnetic moment is in good agreement with the theoretical one ( $7.94\mu_B$ ). The positive Weiss constant indicates the existence of the ferromagnetic coupling of  $\text{Eu}^{2+}$  ions.

The inset of Fig. 5 shows the magnetic susceptibility measured in the applied field of 5 mT. The divergence between the ZFC and FC magnetic susceptibility have been observed below 3.4 K. To clarify this behavior, we measured the field dependence of the magnetization at 1.8 K as shown in Fig. 6. The magnetization linearly increases and then reaches an almost constant value. Actually it still increases with a further increase of the magnetic field strength. The coercive force is very small ( $\sim 1 \text{ mT}$ ). The extrapolation of the high-field magnetic moment to zero field yields a saturation moment of  $6.7\mu_B$ . The magnetic contribution of  $\text{Eu}^{3+}$  to the magnetization of  $\text{Eu}_2\text{CuS}_3$  is negligible at 1.8 K because of its nonmagnetic ground state ( ${}^7F_0$ ). This saturation moment corresponds to the ferromagnetic-ordering magnetization of  $\text{Eu}^{2+}$  which is expected to be  $7\mu_B$ .

The temperature dependence of the specific heat  $C_p$  of  $\text{Eu}_2\text{CuS}_3$  is shown in Fig. 7(a). The sharp  $\lambda$ -type anomaly at 3.4 K indicates that the existence of a long-range magnetic ordering corresponds to the ferromagnetic transition at 3.4 K observed from the magnetic susceptibility. The specific heat of insulating  $\text{Eu}_2\text{CuS}_3$  consists of a magnetic contribution ( $C_{\text{mag}}$ ) and a lattice contribution ( $C_{\text{lat}}$ ). The  $C_{\text{lat}}$  is represented by the usual

harmonic lattice series in odd powers of  $T$ :

$$C_{\text{lat}} = B_3T^3 + B_5T^5 + B_7T^7 + \dots \quad (6)$$

On the assumption that the  $C_{\text{mag}}$  is negligible above 16 K, the constants  $B_3$ ,  $B_5$ ,  $B_7$  were determined by fitting Eq. (6) to the observed specific heat data between 16 and 25 K. The  $C_{\text{mag}}$  is obtained by subtracting  $C_{\text{lat}}$  from the total  $C_p$ . A dashed line in the  $C_p - T$  curve represents the extrapolated specific heat below 1.8 K. This is calculated by fitting to the function  $C_p = BT^{3/2} + C_{\text{lat}}$  in the temperature range  $1.8 \text{ K} \leq T \leq 2.2 \text{ K}$ , because  $C_{\text{mag}}$  for a ferromagnetic ordering is proportional to  $T^{3/2}$  [13]. The temperature dependence of the  $C_{\text{mag}}/T$  and the magnetic entropy calculated by  $S_{\text{mag}} = \int (C_{\text{mag}}/T) dT$  are shown in Fig. 7(b). From the  $S_{\text{mag}} - T$  curve, the magnetic entropy change is estimated to be  $\sim 15 \text{ J mol}^{-1} \text{ K}^{-1}$ , and it is close to  $R \ln(2S+1) = R \ln 8$ .

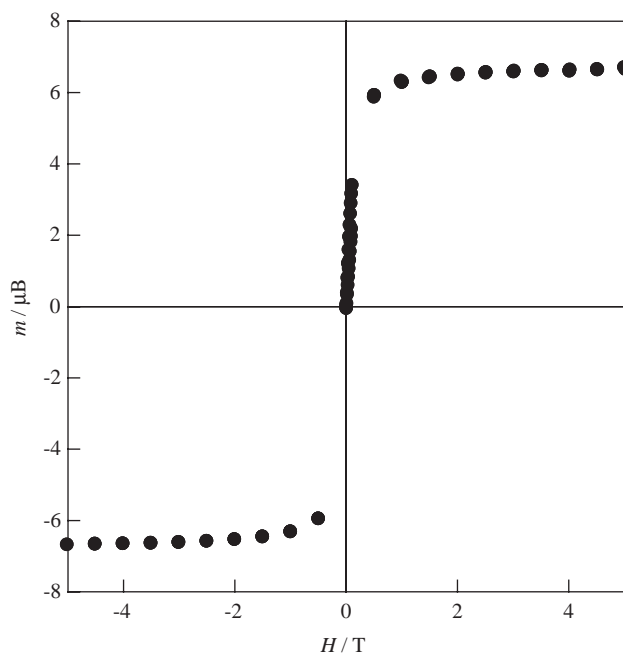


Fig. 6. Field dependence of magnetization measured at 1.8 K for  $\text{Eu}_2\text{CuS}_3$ .

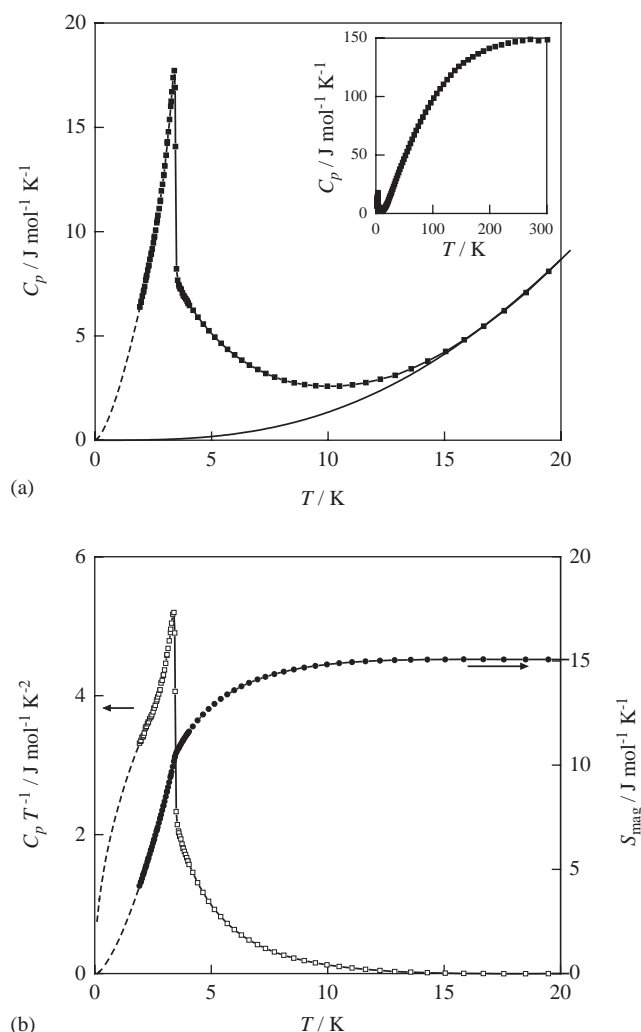


Fig. 7. (a) Temperature dependence of the specific heat below 20 K for  $\text{Eu}_2\text{CuS}_3$ . The inset shows the specific heat behavior up to 300 K. (b) Temperature dependence of the magnetic specific heat divided by temperature (left ordinate) and magnetic entropy (right ordinate) for  $\text{Eu}_2\text{CuS}_3$ .

This result strongly indicates that the ferromagnetic ordering of  $\text{Eu}_2\text{CuS}_3$  is caused by only the  $\text{Eu}^{2+}$  ion and the eight-fold degeneracy remains in the ground state of  $\text{Eu}^{2+}$ , which is consistent with the results obtained through the magnetic susceptibility and the magnetization measurements.

## References

- [1] P. Lemoine, D. Carre, M. Guittard, *Acta Crystallogr. Sect. C: Cryst. Struct. Commun.* 42 (1986) 390.
- [2] R. Pott, G. Guntherodt, *Phys. Rev. B* 27 (1983) 359.
- [3] O. Massenet, J.M.D. Coey, *J. Phys. Colloq. C* 4 (1976) 297.
- [4] M. Wakeshima, Y. Hinatsu, *J. Solid State Chem.* 157 (2001) 117.
- [5] T.I. Volkonskaya, A.G. Gorobets, S.A. Kizhaev, I.A. Smirnov, V.V. Tikhonov, M. Guittard, C. Lavenant, J. Flahaut, *Phys. Stat. Sol. (a)* 57 (1980) 731.
- [6] K.A. Gschneidner Jr., L. Eyring (Eds.), *Handbook on the Physics and Chemistry of Rare Earth*, North-Holland Publishing Company, Amsterdam, 1979 (Chapter 31).
- [7] B.C. Bunker, R.S. Drago, M.K. Kroeger, *J. Am. Chem. Soc.* 104 (1982) 4593.
- [8] F. Izumi, T. Ikeda, *Mater. Sci. Forum* 321–324 (2000) 198.
- [9] N.E. Bresse, M. O'Keefe, *Acta Crystallogr. Sect. B* 47 (1991) 192.
- [10] L. Cario, P. Palvadeau, A. Lafond, C. Deudon, Y. Moëlo, B. Corraze, A. Meerschaut, *Chem. Mater.* 15 (2003) 943.
- [11] U.F. Klein, G. Wortmann, G.M. Kalvius, *J. Magn. Magn. Mater.* 3 (1976) 50.
- [12] J.H. Van Vleck, *The Theory of Electric and Magnetic Susceptibilities*, Clarendon Press, Oxford, 1932, p. 248.
- [13] E.S.R. Gosal, *Specific Heats at Low Temperatures*, Plenum, New York, 1966.